Food Hydrocolloids 145 (2023) 109152

Contents lists available at ScienceDirect

Food Hydrocolloids

journal homepage: www.elsevier.com/locate/foodhyd

Oil structuring through capillary suspensions prepared with wheat middlings micronized directly in oil by high-pressure homogenization

Annachiara Pirozzi [a], Alfredo Posocco [a], Francesco Donsì [a,b,*]

[a] Department of Industrial Engineering, University of Salerno, via Giovanni Paolo II, 132, 84084, Fisciano, SA, Italy
[b] ProdAl scarl, University of Salerno, via Giovanni Paolo II, 132, 84084, Fisciano, SA, Italy

ARTICLE INFO

Keywords:
Oleogel
Capillary suspensions
High-pressure homogenization
Fiber activation
Gel structure
3D network

ABSTRACT

Oleogels have been proposed as suitable systems for replacing unhealthy saturated fats in food preparations. This study aimed to structure sunflower oil through capillary suspensions using wheat middlings (WM), a residue of the wheat milling process, as the solid fraction with structuring properties. For the first time, high-pressure homogenization (HPH) was applied directly to WM dispersed in oil to reduce particle size, activate fibers, and release high-value intracellular compounds into sunflower oil. The optimized formulation of WM-in-oil-suspensions was then used to prepare capillary suspensions by adding water as a secondary immiscible fluid. Water addition drastically altered the rheological behavior and strength of oil suspensions due to the establishment of capillary forces and formation of a percolating particle network. The strength of capillary bridges depended on the particle size distribution and surface properties of WM particles and the fraction of added water (ranging between 5 and 80% v/v with respect to oil). The oil suspension at 30% w/w of HPH-treated WM solid fraction (80 MPa for 20 equivalent passes) with the addition of 50% v/v of water exhibited an apparent "transitional" yield stress >300 Pa, corresponding to gel-like behavior. Additionally, HPH treatment released antioxidant compounds contained in the solid matrix into the system. These results highlight that the resulting capillary suspension is a promising material for formulating healthier and more sustainable food products as an alternative to solid fats, with potential applications based on reduced overall caloric content and added health benefits related to dietary fiber.

1. Introduction

The development of low-fat products has recently become a significant trend in food science, aimed at promoting healthier dietary choices while maintaining palatability and mouthfeel. Several studies have shown a correlation between saturated fat consumption and increased levels of low-density lipoprotein (LDL) cholesterol and apolipoprotein B (ApoB protein) (Liu et al., 2017), which are considered major risk factors for heart disease (Ryoo et al., 2011). Vegetable oil structuring methods have emerged as a promising strategy for reducing or replacing unhealthy (or simply negatively perceived by consumers) solid fats in food products (Hodson et al., 2001). A key requirement for consumer acceptance of food products prepared with fat replacers is that their texture adequately mimics that of regular/full-fat products (Le Révérend et al., 2010). For example, emulsions with adequate droplet size distribution can contribute to reproducing the mouthfeel and stability of full-fat products. Specifically, a widely studied approach to fat replacement involves the use of particle-stabilized Pickering emulsions (Ghosh & Rousseau, 2011; Rousseau, 2000; Rousseau & Hodge, 2005), where droplets cluster together under specific formulations to form spherical agglomerates that maintain excellent stability over time regardless of external environmental stimuli (Pirozzi et al., 2021). It has been demonstrated that adding a small amount of a secondary immiscible fluid to the continuous phase of a particle suspension can create a sample-spanning particle network (Koos, 2014; Mustafa, Pataro, Ferrari, & Donsì, 2018). This phenomenon is attributed to the capillary-bridge forces between the two fluids on solid particles, causing particle agglomeration and, if the mass fraction of solids is sufficient, the formation of a particle network within the bulk fluid (Koos & Willenbacher, 2011). In this case, the rheological properties of ternary solid-liquid-liquid systems are dramatically altered by the transition from a fluid-like to a gel-like state (from a weak to a strong gel) (de Vries et al., 2018; Koos, 2014; Koos & Willenbacher, 2011). This transition in the suspension is associated with two distinct states: the pendular state,

* Corresponding author. Department of Industrial Engineering, University of Salerno, via Giovanni Paolo II, 132, 84084, Fisciano, SA, Italy.
E-mail addresses: apirozzi@unisa.it (A. Pirozzi), a.posocco@studenti.unisa.it (A. Posocco), fdonsi@unisa.it (F. Donsì).

https://doi.org/10.1016/j.foodhyd.2023.109152
Received 21 April 2023; Received in revised form 31 July 2023; Accepted 5 August 2023
Available online 7 August 2023

where the secondary (or minority) fluid preferentially wets particles, for which it has higher affinity than the primary fluid, and the capillary state, where the secondary fluid wets particles less well than the primary fluid (Koos, 2014). Both the capillary state and pendular states are controlled by capillary forces and are strongly influenced by changes in the amount of secondary fluid, material properties, and interfacial and wetting properties of the ternary system (Koos et al., 2012).

For these reasons, capillary suspensions represent a potential alternative route for formulating novel structured food products (Hoffmann et al., 2014) with vegetable oils while reducing the caloric content by replacing part of the fats with a secondary fluid, such as water, and solid particles, such as fibrous materials (Principato et al., 2021).

In this context, various agri-food residues (AFRs), such as tomato peels and spent coffee grounds (Mustafa et al., 2018), and different fractions of yellow pea processing residues (Calabrese et al., 2021), have demonstrated excellent ability to structure vegetable oils (Ferrari et al., 2017), through the addition of a small amount of secondary immiscible fluid.

This study presents significant contributions and introduces several novel aspects in structuring vegetable sunflower oil, specifically through the formation of gel-like products using wheat middlings (WM). WM, fine particles derived from the endosperm of wheat, possess a high fiber content and are typically utilized as animal feed due to their abundant energy, amino acid, and phosphorus content (Galanakis, 2018; Q. Huang et al., 2014; Rosenfelder et al., 2013). By valorizing these AFRs, this research contributes to the implementation of the circular economy within the food chain.

A unique and innovative aspect of this study lies in the investigation of the network formation mechanism of WM particles when micronized using high-pressure homogenization (HPH) and suspended directly in oil. This approach enables the treatment of high concentrations of WM without the clogging of the HPH orifice valve, thereby allowing for the creation of structured low-calorie food products with improved texture and stability, effectively mimicking full-fat products. Remarkably, these structured food products can be achieved without the need for unhealthy fats or undesired additives, with water as the secondary immiscible fluid.

Moreover, the utilization of WM in the structuring of vegetable oil offers an additional advantage in terms of potential health benefits and flavor enhancement. To explore this aspect, the study delves into the potential of HPH-micronized WM particles to attenuate lipid oxidation, a critical factor in enhancing the shelf life and overall quality of food products. By exploiting WM's natural antioxidant properties, the research aims to contribute to the development of healthier and more nutritious food alternatives.

2. Materials and methods

2.1. Raw materials

The wheat middlings (WM), collected from a local milling industry (Molini Giardullo Di Giardullo Silvia E C. S.n.c., Albanella (SA), Italy), were packed in vacuum-sealed flexible pouches (multilayer packaging OPP30-A19-LDPE70, Di Mauro Officine Grafiche S.p.A., Cava de' Tirreni (SA), Italy) and stored at room temperature until used. The moisture content of WM was 11.54 ± 0.10%.

Sunflower oil was purchased from a local market (Olio di Semi di Girasole Basso, San Michele di Serino (AV), Italy). Its composition (on weight basis) comprises 10.3% wt of saturated fatty acids, 19.5% wt of monounsaturated fatty acids, and 65.7% wt of polyunsaturated fatty acids, as stated on the product label.

Folin-Ciocaleau's Reagent (1.8–2.2 mol/L, PanReac, Barcelona, Spain), sodium carbonate ($NaCO_3$, ACS GR, PanReac, Barcelona, Spain), TPTZ (2,4,6-Tris (2-pyridil)-*s*-triazine, ≥99.0%, Sigma-Aldrich, St. Louis, MO, USA), chloridric acid (HCl, 36.5–38.0%, ACS GR, PanReac, Barcelona, Spain), and iron (III) chloride hexahydrate ($FeCl_3{\cdot}6H_2O$, ≥98%, Sigma-Aldrich, St. Louis, MO, USA) were used as received without further purification. All water used throughout this work was purified by Milli-Q water purification system (Barnstead™ Pacific TII Water, Thermo Scientific, Waltham, MA, USA).

Table 1
WM-in-water or WM-in-oil suspensions prepared, with the indication of sample name, continuous phase used, solid fraction and applied milling treatment.

Sample	Continuous phase	Solid fraction φ (% w/w)	Mechanical treatment	Fractional water holding FWH (%)	Fractional oil holding FOH (%)
HSM-O-φ1	Sunflower oil	5	HSM	-	742.2
HSM-O-φ2	Sunflower oil	15	HSM	-	221.4
HSM-O-φ3	Sunflower oil	20	HSM	-	156.3
HSM-O-φ4	Sunflower oil	25	HSM	-	117.2
HSM-O-φ5	Sunflower oil	30	HSM	-	91.2
HPH-O-φ1	Sunflower oil	5	HSM + HPH	-	754.0
HPH-O-φ2	Sunflower oil	15	HSM + HPH	-	224.9
HPH-O-φ3	Sunflower oil	20	HSM + HPH	-	158.7
HPH-O-φ4	Sunflower oil	25	HSM + HPH	-	119.1
HPH-O-φ5	Sunflower oil	30	HSM + HPH	-	92.6
HSM-W-φ1	Water	5	HSM	424.1	-
HPH-W-φ1	Water	5	HSM + HPH	840.7	-

2.2. Chemical composition of wheat middlings

The chemical composition of WM was determined by applying official analytical methods. Moisture and ash content were evaluated by drying at 105 °C in an air-force oven (950.46 AOAC), and at 525 °C in a muffle (923.02 AOAC), respectively; total protein was determined by the Kjeldahl method (954.01 AOAC); total fat was quantified by gravimetry after extraction with a mixture of petroleum ether and diethyl ether (1:1) (920.39 AOAC).

The extractives, cellulose, hemicelluloses and lignin content were determined using the gravimetric method according to the Technical Association of Pulp and Paper Industry (TAPPI) methods. More in detail, during the first isolation step, the extractive content was determined through the TAPPI method (T-264 om-82) (Tappi, 2007) and ASTM E1721-01, using a Soxhlet apparatus to remove sugars, phenolic compounds, and part of water-soluble polysaccharides. Lignin extraction was based on the TAPPI T-222 om-22 methodology (Tappi, 2006), according to which the obtained extractive-free sample was subjected to acid hydrolysis. Cellulose extraction, based on the TAPPI T-203 method, was obtained by alkaline treatment with soda and acetic acid applied on extractive-free samples from the first isolation step.

2.3. Preparation of wheat middlings suspensions by mechanical treatments

WM particles were dispersed in sunflower oil at a solid mass fraction (φ, defined as the ratio of the solid weight to the total sample weight) ranging between 5 and 30% w/w, using a high-shear mixer (HSM) (Ultra Turrax T25, IKA Labortechnik, Germany) at 20,000 rpm for 5 min within an ice bath. The obtained suspensions were then subjected to high-pressure homogenization (HPH) treatment at 80 MPa for 20

equivalent passes using an in-house developed system equipped with a 200 μm diameter orifice valve (model WS1973, Maximator JET GmbH, Schweinfurt, Germany) and a tube-in-tube heat exchanger, to avoid the increase in product temperature, using cooling water at 10 °C.

WM particles were also dispersed in water at φ = 5% w/w by HSM and, subsequently, treated by HPH under the same conditions described for oil suspensions, to investigate the effect of different process media on micronization efficiency. The lower solid fraction used in water was required to avoid the HPH valve clogging, which, instead, did not occur at the higher WM fractions tested in oil.

Table 1 summarize the treatments carried out on oil and water suspensions and the abbreviations used.

2.4. Characterization of water and oil suspensions

2.4.1. Bioactivity determination

Total phenols were determined through the Folin-Ciocalteau assay (Slinkard & Singleton, 1977). Briefly, 1 mL of WM suspensions in distilled water, prepared by HSM or HPH (HSM-W-φ1 and HPH-W-φ1) were added to Folin-Ciocalteau's reagent (5 mL at 10% v/v) and allowed to stand for 5 min at room temperature. Then, 4 mL of sodium carbonate solution at 7.5% w/v was added to the mixture. After vortexing for 1 min, the mixture was incubated at room temperature for 50 min in darkness. The reacting mixture was then centrifuged at 5,300×*g* equivalent force for 10 min at 25 °C and the absorbance was read at 765 nm using a V-650 UV–Vis Spectrophotometer (Jasco Inc., Easton, MD, USA). Total phenols were expressed as milligrams of gallic acid equivalents per gram of dry middlings (mg_{GAE}/g_{DM}), employing the calibration curve obtained with a gallic acid standard at different concentrations (10–100 mg/L).

The reducing capacity of the suspensions was evaluated using the FRAP (ferric reducing antioxidant power) assay (Benzie & Strain, 1996). The freshly-prepared (Pirozzi et al., 2022) FRAP reagent solution (2.5 mL) was mixed with 0.5 mL of opportunely diluted samples and incubated for 10 min at ambient temperature. The absorbance of the reacting mixture after centrifugation (relative centrifugal force of 5,300×*g* for 10 min at 25 °C) was measured at 593 nm using a V-650 UV–Vis spectrophotometer (Jasco Europe Srl, Cremella, Italy) against a blank sample. Ascorbic acid was used as the standard for the calibration curve and the FRAP values were expressed as ascorbic acid equivalents present in the dry analyzed sample (mg_{AAE}/g_{DM}).

2.4.2. Size distribution of the suspensions

The particle size distribution of the samples micronized by HSM or HPH was measured by laser diffraction using a Malvern Mastersizer 2000 (Malvern Instruments Ltd., UK). WM-in-water suspensions were analyzed as prepared; in contrast, for WM-in-oil suspensions, the oil phase was replaced by water by washing three times the suspensions with saponin from Quillaja bark (Sigma-Aldrich, St. Louis, MO, USA) at 0.5% w/v in water, followed by centrifugation at 5,300×*g*. From the particle size distribution, the diameters corresponding to the 10th, 50th and 90th percentile of the cumulative distribution (d(0.1), d(0.5) and d (0.9), respectively), the volume-based mean diameter (D[4,3]), the surface-based mean diameter (D[3,2]), and the relative span factors were calculated, as previously described (Pirozzi et al., 2021). The temperature of the cell was maintained at 25 ± 0.5 °C, and the mean value of three independent replicates was determined.

2.4.3. Water and oil holding capacity

The hydration and oil binding properties of WM particles are related to their chemical structure and particle size (Fleury & Lahaye, 1991). The particle swelling was determined according to a previously reported method (Calabrese et al., 2021). Briefly, WM was dispersed in distilled water at two different concentrations (5 and 7% w/w) and allowed to swell overnight under continuous stirring at 20 °C. Then, 2 g of each aqueous suspension was centrifuged for 30 min at 25 °C and 1,626×*g* and, after removing the supernatant, the pellet was weighed. The maximum amount of water retained per g of WM (WH_{max}) was calculated as the average of each WM concentration used (determined in triplicate independent experiments):

$$WH_{max}\left(\frac{g_{water}}{g_{WM}}\right)=\frac{\sum_{i=1}^{3}\frac{P_{water,i}-SC}{SC}}{3} \quad \text{(Eq. 1)}$$

where $P_{water,i}$ is the weight of the pellet after centrifugation of each WM suspension in water and *SC* is the solid content of the sample (g).

The fractional water holding (FWH) was defined as the capacity of middlings particles to retain water when in the oil-water capillary suspension, expressed as:

$$FWH\ (\%)=\frac{100\bullet\left(\frac{WC}{SC}\right)}{WH_{max}} \quad \text{(Eq. 2)}$$

where *WC* is the water content (g).

When the FWH value is lower than 100%, the solid content is exposed to less water than its maximum holding capacity (corresponding to 100%); in contrast, for FWH higher than 100%, the particles have been exposed to excess water compared to their holding capacity.

The same procedure was carried out to determine the maximum oil holding capacity (OH_{max}) and the fractional oil holding (FOH).

$$OH_{max}\left(\frac{g_{oil}}{g_{WM}}\right)=\frac{\sum_{i=1}^{3}\frac{P_{oil,i}-SC}{SC}}{3} \quad \text{(Eq. 3)}$$

$$FOH\ (\%)=\frac{100\bullet\left(\frac{OC}{SC}\right)}{OH_{max}} \quad \text{(Eq. 4)}$$

where OH_{max} is the maximum oil holding capacity calculated, P_{oil} is the weight of pellet after centrifuging the suspension of particles in oil (g), and *OC* is the oil content (g).

2.4.4. Three-phase contact angle

The structure of capillary suspensions and their strength depends on the particle size distribution, as well as on the interfacial tension between the fluids (Bossler et al., 2017) and the wetting properties of both liquids, which are all taken into account by the three-phase contact angle measurement (Koos et al., 2012). The three-phase contact angle was measured for HSM-O-φ5 and HPH-O-φ5 with the sessile drop method, as previously described (Hoffmann et al., 2014), using a contact angle meter (CAM 200, KSV Instruments Ltd., Helsinki, Finland). Each suspension was placed in a quartz cuvette and left for 24 h at room temperature to allow gravitational separation of the solid particles from the oil phase. Subsequently, the secondary fluid (distilled water) was placed in a 500 μL syringe (Hamilton Company, Bonaduz, Switzerland) with a 0.72 mm diameter stainless steel needle, to form a drop of about 2 μL in the cuvette filled with the oil phase for two-third of its volume and with the solid particles onto the bottom. Drop formation triggered the activation of a camera, which recorded the shape of the drop once deposited on the particle layer for 100 s at 1 s time intervals. An image analyzer software (CAM 101, KSV Instruments Ltd., Helsinki, Finland) was used to measure the angle formed between the surface in contact with the drop, and the tangent to the drop of liquid at the point of contact with the surface, on both sides of the image. For each drop formed, values of the contact angles were averaged over time and side. Measurements were repeated five times for each sample. Results are expressed as an average of the values during the 100 s.

2.5. Preparation of capillary suspensions

The capillary suspensions were obtained by adding dropwise distilled water as a secondary fluid at saturation ratio S (Equation (5)) comprised between 0.05 and 0.70 v/v to the HSM- or HPH-treated WM-in-oil suspensions at constant particle volumetric fraction φ = 30% w/w

Table 2
Chemical composition of the wheat middlings used in this work.

WM component	WM percentage composition (wt %) on dry basis (except for moisture)
Moisture content	10.59 ± 0.01
Ash content	3.79 ± 0.25
Protein	18.53 ± 1.21
Fat	0.82 ± 0.04
Extractives	10.37 ± 0.63
Cellulose	14.74 ± 1.68
Hemicellulose	38.31 ± 0.95
Lignin	5.67 ± 0.93

(HSM-O-φ5 or HPH-O-φ5) under HSM at 20,000 rpm for 10 min within an ice bath (Bossler et al., 2017).

$$S = \frac{V_{water}}{V_{oil} + V_{water}} \quad \text{(Eq. 5)}$$

2.6. Light microscopy analysis

The morphology of suspensions in oil and capillary suspensions was observed with an optical microscope (Nikon Eclipse TE 2000S, Nikon instruments Europe B.V., Amsterdam, The Netherlands), coupled to a DS Camera Control Unit (DS-5M-L1, Nikon Instruments Europe B.V, Amsterdam, The Netherlands) for image acquisition and analysis.

2.7. Rheological analysis

Rheological measurements were performed in a rotational rheometer (AR 2000 rheometer, TA instruments, Newcastle, DE, USA), equipped with a concentric cylinder (15 mm stator inner diameter, 28 mm rotor outer diameter, 42 mm cylinder immersed height, 2° cone angle) and plate-cone geometry (40 mm diameter, 2° cone angle and 1 mm fixed gap width) based on the sample to be analyzed. The apparent yield stress, i.e. the stress at which the sample begins to flow, is generally evaluated using a shear rate ramping, by finding the intercept point between the y-axis and a tangent line into the stress vs. shear rate curve at the point where the curve slope does not significantly change as the shear rate increases. However, since the yield stresses in tested materials do not exhibit a well-defined yield plateau, the apparent "transitional" yield stress was identified as the point at which the slope of the logarithmic deformation as a function of the logarithmic shear stress changes. Flow curves were obtained by continuously varying the shear rate from 0.1 s^{-1} up to a rate of 200 s^{-1} at 20 °C. Measurements were repeated five times on two independently prepared samples, and are reported as means ± standard deviations for apparent transitional yield stress.

2.8. Statistical analysis

All experiments and analysis were performed in triplicate on independently prepared samples, unless otherwise specified, and the mean and standard deviation (SD) of the experimental values were calculated. Statistically significant differences ($p \leq 0.05$) among the mean values were assessed by one-way ANOVA and the Tukey's test ($p < 0.05$), using statistical software SPSS (version 20, SPSS Inc., Chicago, IL, USA).

3. Results and discussion

3.1. Chemical composition of wheat middlings

Table 2 reports the chemical composition of WM as a percentage of dry weight. The composition is reported to vary depending on the wheat variety, environmental factors during production and storage, and processing techniques used (Q. Huang et al., 2014).

WM mainly consist of non-starch polysaccharides, dietary fibers, and proteins, with low lipid content. This composition aligns with previous findings (Cromwell et al., 2000; Q. Huang et al., 2014; Kosseva, 2020). Notably, the presence of surface-active non-starch polysaccharides (Goh et al., 2014; Yue et al., 2008), in combination with dietary fibers, i.e. the mixture of complex organic substances including cellulose, hemicellulosic components, lignin, and pectin (Stevenson et al., 2012), and protein materials (Bagnasco et al., 2013), is known to play a pivotal role in forming 3D-networks and stabilizing food matrices. Additionally, these components contribute to structuring various food systems (De

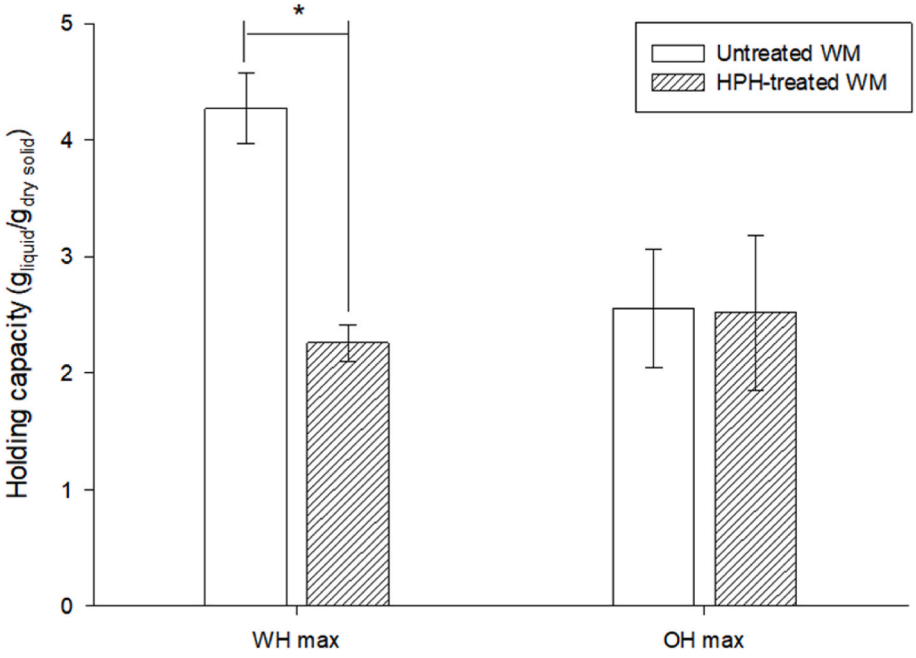

Fig. 1. Water (WH_{max}) and oil holding capacity (OH_{max}) of untreated and high-pressure homogenized wheat middlings. Asterisk represents significant differences at $p < 0.05$.

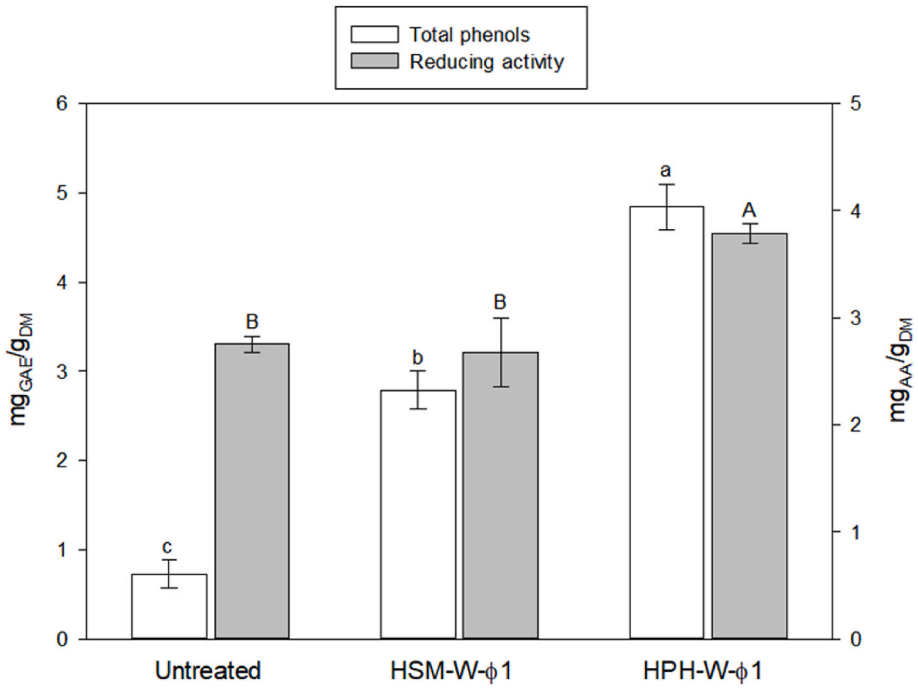

Fig. 2. Total phenolic content (milligrams of gallic acid equivalents per gram of dry WM, mg_{GAE}/g_{DM}) and reducing capacity (milligrams of ascorbic acid equivalents per gram of dry WM, mg_{AAE}/g_{DM}) of WM-in-water-suspensions at $\varphi = 5\%$ w/w upon different treatments. Different lowercase letters indicate significant differences ($p < 0.05$) within the total phenols analysis. Different uppercase letters indicate significant differences ($p < 0.05$) within the reducing activity analysis.

Vasconcelos et al., 2013), through the formation of polysaccharide-protein complexes (Bealer et al., 2020; Stanton et al., 2018). Consequently, WM shows great promise as a natural material for use as a structuring agent in 3D capillary suspension networks, contributing to the development of the desired texture and stability.

3.2. Water and oil holding capacities

Water and oil holding capacities describe the ability of solid particles to adsorb and retain respectively water and oil, which is bound or entrapped through hydrodynamic, capillary, and physical interactions (Damodaran & Paraf, 2017). WM particles are very rich in starch and fibers, especially cellulose, which positively influences water adsorption, whereas the presence of natural oil, wax, and fat hinders water molecules from penetrating inside the fibers (Begum et al., 2021). The maximum water holding capacity WH_{max} measured for WM was 4.5 ± 0.3 g_{water}/g_{WM}, suggesting that water is able to fill the void space of the WM anisotropic particles, which is important, as high water penetration was reported to play a key role in structuring capillary suspension of starch particles (Hoffmann et al., 2014). Solid particles with high water-holding capacity, such as WM, can function as ingredients to limit synaeresis and control viscosity and texture in formulated foods (Grigelmo-Miguel & Martín-Belloso, 1999). WM exhibited a maximum oil holding capacity OH_{max} of 2.8 ± 0.9 g_{oil}/g_{WM}, which is only half the value of its maximum water holding capacity.

Water and oil holding capacities (WHC and OHC) measure a material's ability to retain water and oil after centrifugation (Equations (2) and (4)). A material's water holding capacity is closely related to its dietary fiber content. The hydration properties of dietary fibers depend on factors such as the chemical structure of polysaccharides, porosity, particle size, ionic form, pH, temperature, ionic strength, type of ions in solution, and stresses on fibers (Elleuch et al., 2011). WM particles have a high fiber content and, therefore, exhibit high maximum water holding capacity (WH_{max}). Maximum oil holding capacity (OH_{max}) is closely related to the chemical structure of plant polysaccharides and depends on factors such as surface properties, charge density, particle size, insoluble fiber content, and the hydrophobic nature of the fiber particle (L. Huang et al., 2020).

HPH treatment causes the micronization of WM, altering their physical structure due to the applied fluid-mechanical stresses. This affects WM's water and oil holding capacities, which are related to the structure, density, and the number of the available water and oil-binding sites. HPH treatment caused a significant reduction in particle size of WM dispersed both in water and oil increasing surface area and exposing more water-binding sites (polar or uronic acid groups) to surrounding water (Chen et al., 2013), hence increasing WH_{max} value (Chau et al., 2007). However, the obtained results (Fig. 1) suggest that fluid-mechanical stresses from HPH treatment, including shear, elongation, turbulence, and hydrodynamic cavitation (Coccaro et al., 2018; Pirozzi et al., 2021) are responsible not only for cell break-up, but also for fiber activation, by causing the fiber matrix and pores of WM to collapse, negatively affecting the hydration properties of WM particles (Hu et al., 2015). HPH treatment appears to have diminished the exposure of WM's hydrophilic groups while enhancing mutual fiber attraction, leading to a lower WH_{max} for HPH-treated samples in comparison to untreated ones (Fig. 1). However, it is important to note that HPH treatment did not affect the physical entrapment of oil and, as a result, did not impact the oil holding capability of the samples.

The values for FWH and FOH in the different capillary suspension formulations are reported in Table S1 of the Supplementary Material, showing for which formulations defect or excess water or oil are used.

3.3. Wheat middlings-in-water-suspensions

WM particles contain various phytochemicals, including phenolic compounds with high reducing activity, as shown in Fig. 2. The impact of processing methods, such as HSM and HPH treatments, on the total phenolic content and reducing activity of WM-in water-suspensions at a concentration of $\varphi = 5\%$ w/w is illustrated in Fig. 2.

Under identical extraction conditions, (time, temperature, and solid-liquid ratio), the treatment applied significantly impacted the extraction efficiency of total phenols and their associated reducing activity. The

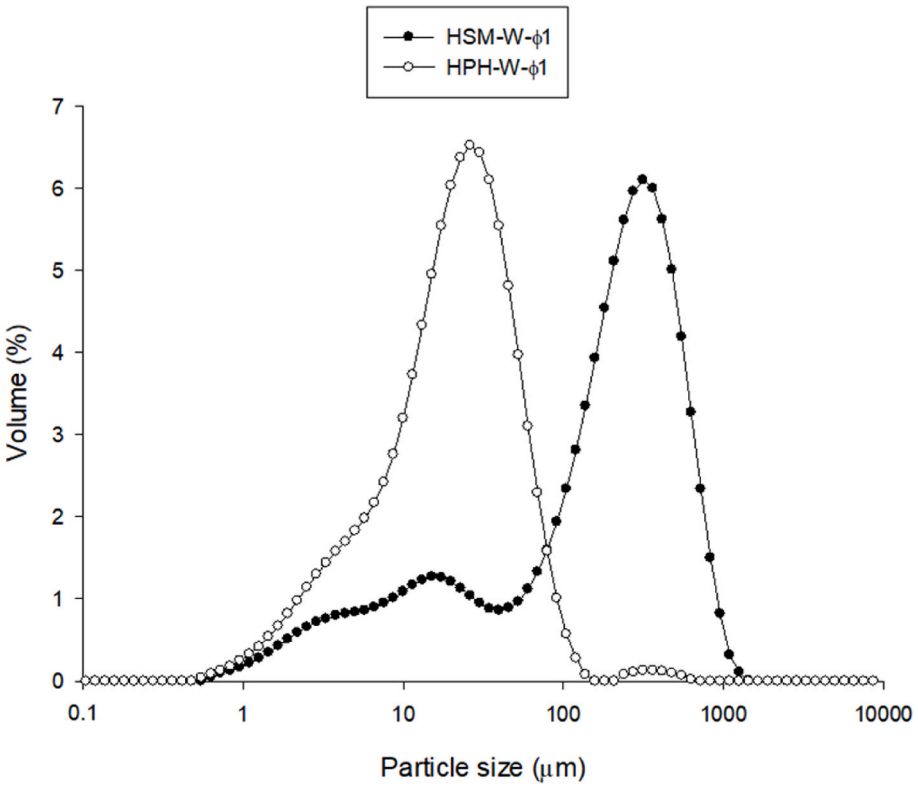

Fig. 3. Particle size distribution of WM-in-water-suspensions treated by high-shear mixing (HSM-W-φ1) and high-pressure homogenization (HPH-W-φ1).

Table 3
Effect of different mechanical treatments of WM-in-water-suspensions on particle size distribution (expressed as span and characteristic diameters).

Characteristic diameters (μm)	HSM	HPH
d(0.1)	8.55	4.40
d(0.5)	220.64	22.62
d(0.9)	595.37	59.55
Span (-)	2.66	2.44
D[4,3]	266.08	30.68
D[3,2]	21.80	10.43

HSM treatment resulted in a 285% increase in phenols extraction yield, compared to the untreated sample. Additionally, combining HSM and HPH treatments further enhanced phenols extraction yield, with total phenolic content increasing from 2.79 ± 0.21 mg_{GAE}/g_{DM} after HSM to 4.84 ± 0.25 mg_{GAE}/g_{DM} after HPH (+74%). The results indicate that HPH positively impacts the extraction of phenolic acids from WM, due to the decreased size dimensions and consequentially increased surface area, and a faster diffusion facilitated by the smaller particle size resulting from the homogenization process. This results in high antioxidant activity, which helps maintain the quality of sunflower oil in capillary suspension against oxidation throughout the storage period (see Fig. S1 in Supplementary Material).

It is important to note that HSM did not affect the reducing activity; no significant difference was observed compared with the untreated sample. However, applying HPH immediately after HSM, significantly increased the reducing activity of WM-in-water-suspensions by 41%, as measured by the FRAP method, from 2.68 ± 0.32 mg_{AAE}/g_{DM} to 3.78 ± 0.09 mg_{AAE}/g_{DM}.

As previously mentioned, the increased release of intracellular compounds, such as polyphenols, is dependent on size reduction, as indicated by the particle size distribution curves shown in Fig. 3.

The sample treated with HSM exhibited a bimodal particle size distribution, with sizes ranging from 1 to 1,000 μm. However, HPH treatment effectively reduced the size of WM particles, resulting in a more uniform and narrower size distribution profile (ranging from 1 to 100 μm). At 80 MPa, HPH significantly decreased the d(0.5), D[4,3] and D[3,2] values by approximately 90%, 88%, and 52%, respectively, compared to the HSM-treated sample (Table 3). These results suggest

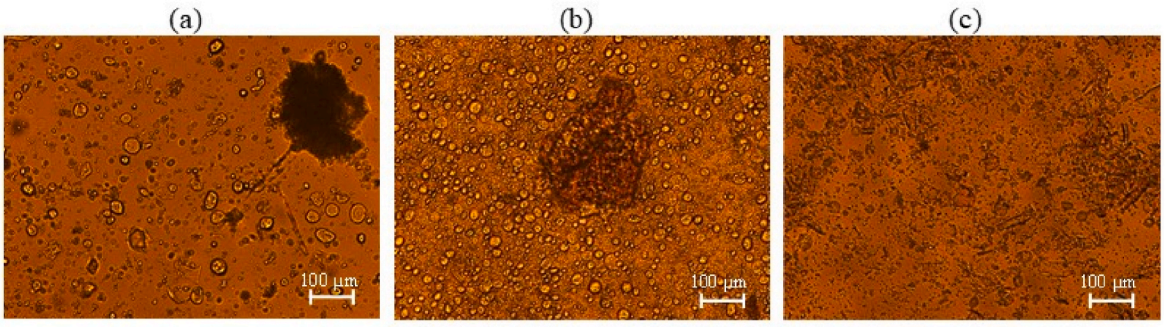

Fig. 4. Optical microscopy at 10x magnification for untreated (a), HSM (b) and HPH (c) treated WM-in water-suspensions.

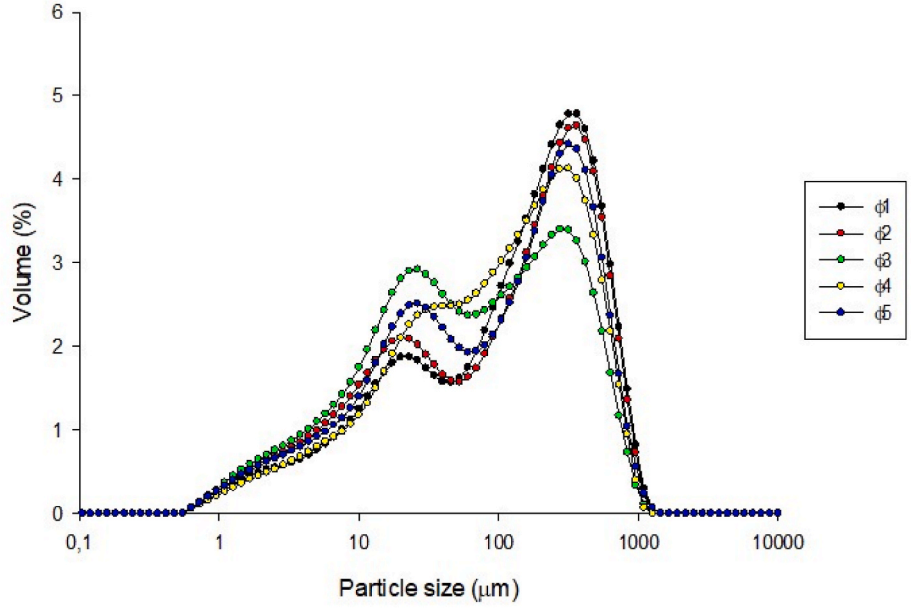

(a)

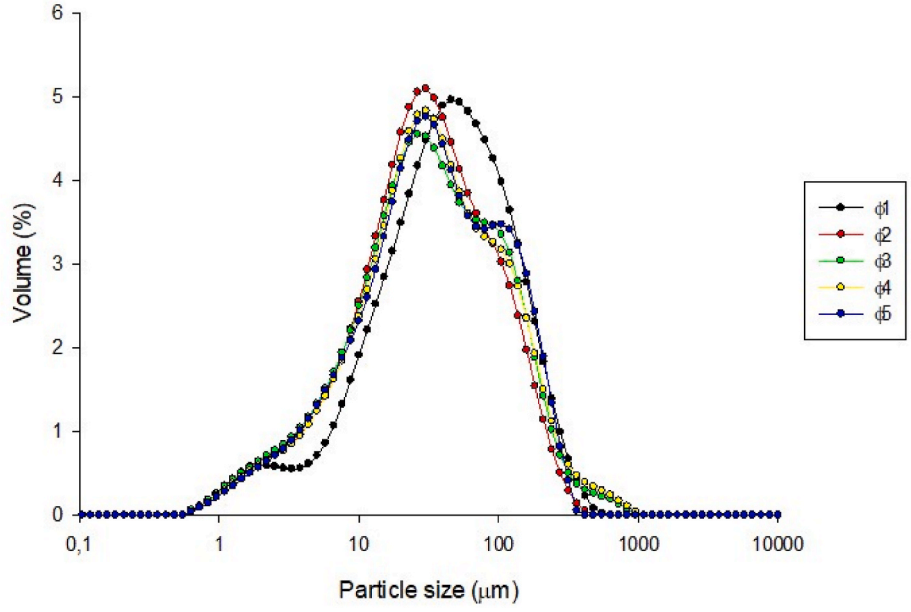

(b)

Fig. 5. Particle size distribution of WM-in-oil-suspensions treated with high-shear mixing (a) and high-pressure homogenization (b) at different particle mass fractions (φ).

that the fluid-mechanical stresses generated in the homogenization valve during the HPH process disrupted WM dispersed in water, producing a WM suspension with smaller suspended particles. The D[4,3] values for HSM and HPH were 266.1 μm and 30.7 μm, respectively, while the D[3,2] values were 20.8 μm and 10.4 μm for HSM and HPH, respectively. Given that the D[4,3] is greatly influenced by large particles and D[3,2] is more influenced by smaller ones, these results indicate a significant increase in the number of small particles when WM was homogenized.

The reduction in particle size observed is consistent with the increase in extraction yield of phenols. Specifically, the one log reduction in mean particle size due to HPH treatment resulted in a doubling of total phenols extraction yield compared with HSM. A size distribution below the typical plant cell size (~100 μm) suggests successful cell disruption (Jurić et al., 2019), which facilitates the recovery of intracellular compounds with high yields.

Fig. 4 shows micrographs of untreated and treated WM suspensions that support these observations.

Consistent with particle size measurements, the untreated sample (Fig. 4a) contained a large number of particles and exhibited higher agglomeration. The sample treated with HSM (Fig. 4b) exhibited better dispersion but showed only a slight size reduction, likely due to particle deagglomeration. In contrast, HPH treatment (Fig. 4c) led to material fragmentation, resulting in the dispersion of cell wall fragments, cellular

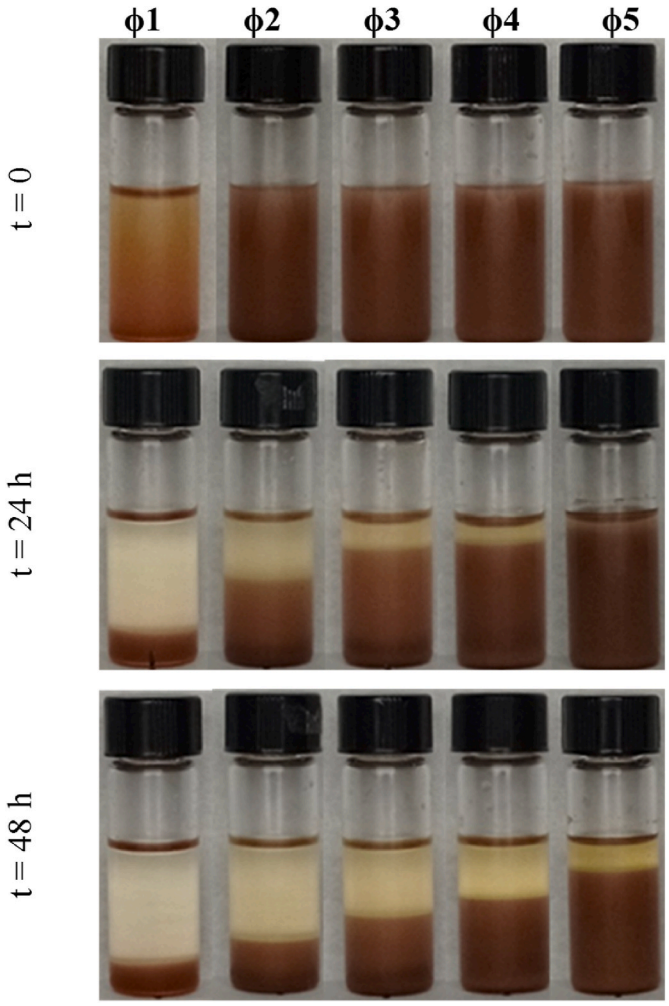

Fig. 6. Pictures of the different WM-in-oil-suspensions prepared by HPH treatment, after 0, 24 and 48 h.

material, fiber particles and polymers in water. Subsequently, the HPH treatment exposed and released soluble components from the WM particles (e.g., phenols, as shown in Fig. 2), while the insoluble fraction underwent mechanical defibrillation, transforming into a fibrous material (Yuan et al., 2023) (Fig. 3c).

In summary, Figs. 3 and 4 demonstrate that HPH treatment significantly reduced the particle sizes of WM samples. This plays a crucial role in increasing the surface area and facilitating the rapid diffusion and release of intracellular material in suspension.

3.4. Wheat middlings-in-oil-suspensions

Particle size and shape play important roles in determining the rheological properties of oil suspensions (Mewis & Wagner, 2011).

Interestingly, the particle size distribution of WM-in-oil-suspension at φ1 differs slightly from the WM-in-water-suspension at the same particle mass fraction. This may be due to the procedure used for particle size analysis of oil suspensions, which involves removing the oil by washing the sample three times with distilled water and surfactant. However, it is also possible that the different affinity of WM for water and oil, as indicated by their water and oil holding capacities, may have affected the impact of the HPH process on particle disruption (Su et al., 2019). Specifically, when WM particles are processed in water, a greater reduction in particle size is achieved with HPH process due to the larger volume of particles when wetted with water, resulting from WM's higher water-absorbing ability compared to oil.

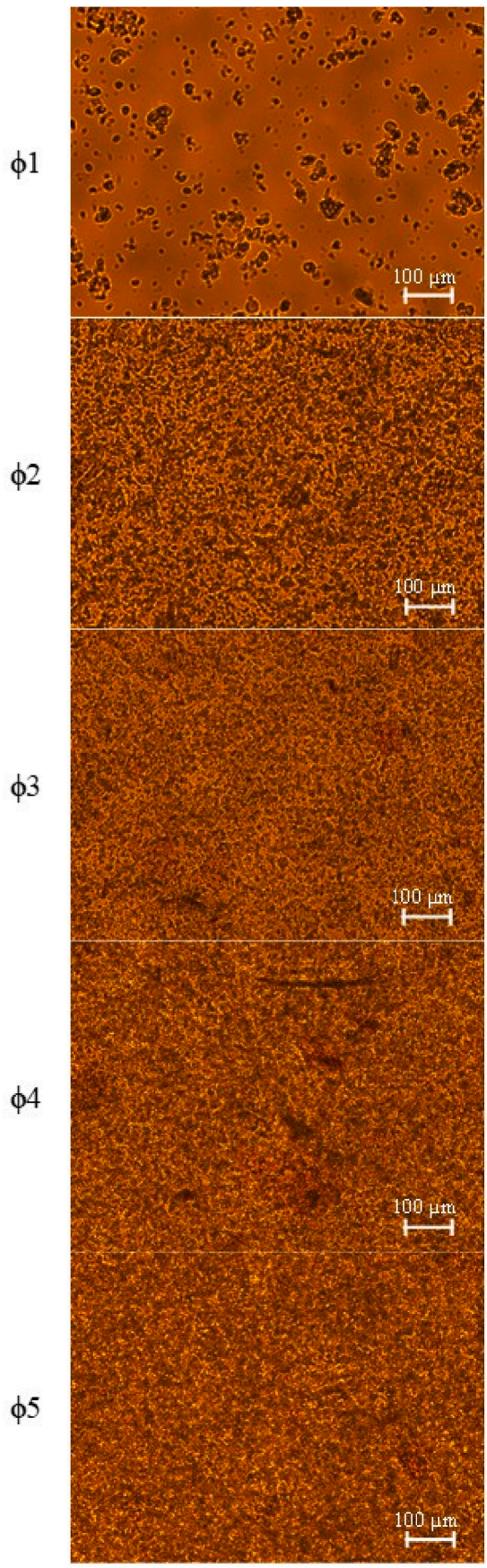

Fig. 7. Optical micrographs at 10x magnification for HPH treated WM-in oil-suspensions at different mass fractions.

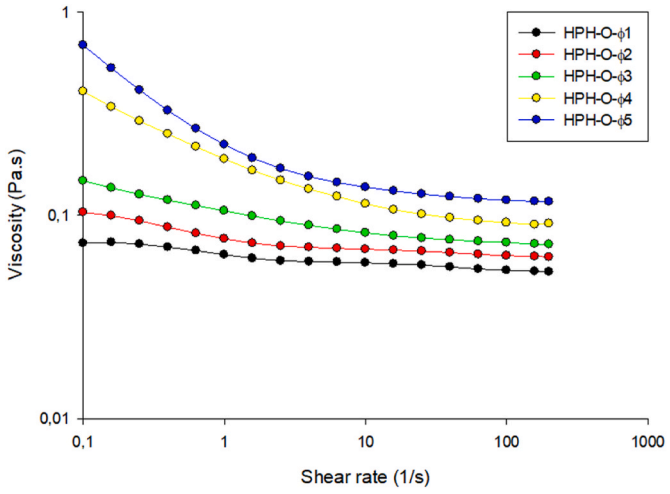

Fig. 8. Flow curves for HPH treated WM-in-oil-suspensions at different particle mass fractions φ.

Due to the significant impact of the sample preparation procedure on size distribution, the particle size distribution for WM-in-oil-suspensions treated with HSM and HPH, shown in Fig. 5a and b respectively, should be considered only as qualitative analyses that provide information on the effects of the two different mechanical treatments on oil suspensions. The WM-based oil suspensions produced with HPH exhibited a narrower and more homogeneous distribution than HSM-treated samples for all tested particle mass fractions, with reductions of approximately 14%, 68% and 71% for the 10th, 50th and 90th percentile of the cumulative distribution, respectively. The HSM-treated WM-in-oil-suspensions displayed a bimodal distribution with a peak at approximately 450 μm and a broader shoulder at a smaller size of approximately 20 μm (Fig. 5a). In contrast, the particle size distribution of HPH-treated WM-in-oil-suspensions showed a dominant size at approximately 20 μm with only a minor shoulder at a larger size, indicating that WM particles were broken down into cell wall fragments, cellular material, fiber particles and polymers by the HPH treatment even in oil.

The ability of WM particles to structure the oil phase was initially evaluated through visual observations (Fig. 6) immediately after HPH treatment and after leaving the oil suspensions at room temperature for 24 h and 48 h.

WM-in-oil-suspensions exhibited varying degree of sedimentation depending on the particle mass fraction, as shown in Fig. 6. At φ1, most solid particles settled at the bottom of the vials within 24 h. As the particle mass fraction increased, sedimentation took longer due to strong interparticle interactions (Shajahan & Paul, 2020). At φ5 (30% w/w of WM particles), the oil suspension had a more homogeneous, paste-like appearance, suggesting that the continuous oil phase lubricated the particles. Notably, although at φ5, the OH_{max} value is reached (FOH ~ 91%, see Table 1), there is still some degree of settlement in the WM, albeit to a lesser extent than observed in the other samples, characterized by FOH ≫ 100% (Table 1).

Samples with a higher particle concentration exhibited greater kinetic stability due to the formation of a densely packed particle network, as illustrated in Fig. 7. The tightly packed arrangement and interlocking of particles in these samples resulted in enhanced resistance to sedimentation. Thus, this phenomenon can be attributed to the increased frequency of particle-particle interactions and the formation of physical barriers, which collectively contributed to the overall kinetic stability of the system.

Fig. 7 clearly illustrates the difference between φ1 and φ2 (5% and 15% w/w particle mass fraction, respectively), where at φ1 particle interaction resulted in well-separated aggregates, while at φ2 a network structure developed. This network appears to become stronger with increasing particle fraction, as suggested by the rheological properties of WM-oil-suspensions shown in Fig. 8.

Table 4
Fitting parameters and coefficients of determination for the fitting of the data of Fig. 8, using Equation (6).

	k (Pa·s^n)	n (-)	R^2	Adj-R^2
φ1	0.06	1.00	n.a.	n.a.
φ2	0.08	1.05	0.7517	0.7399
φ3	0.11	1.13	0.9698	0.9684
φ4	0.19	1.36	0.9834	0.9826
φ5	0.25	1.46	0.9848	0.9840

n.a.: not available because the HPH-O- φ1 curve is not adequately fitted by a power-law model.

The results of the shear-controlled tests (Fig. 8 and Figure S2a) indicate that the flow curves of WM-in-oil-suspensions are characterized by an increase in viscosity (η) as a function of the particle mass fraction. Specifically, the shape of the fluid curves transitions from Newtonian-like behavior, where viscosity is independent of shear rate, to non-Newtonian shear-thinning response, where viscosity decreases with increasing shear rate. This shear-thinning behavior can be attributed to the breakage of the aggregates, changes in particle shape, and particle orientation in the flow direction, as observed for pea fiber suspensions in oil (Calabrese et al., 2021). This behavior had been previously fitted using the power-law model of Equation (6) (Calabrese et al., 2021):

$$\eta = k\,\dot{\gamma}^{1-n} \qquad \text{(Eq. 6)}$$

with n representing the power-law index (-) and k that is the consistency factor (Pa·s^n).

In Equation (6), the value of n describes the behavior of a non-Newtonian fluid: if $0 \leq n < 1$, the fluid is shear-thickening, while if $n > 1$ the slope of $\eta(\gamma)$ curves will have a negative shape and the fluid is shear-thinning. For all WM-in-oil-suspensions, the power-law index is greater than or equal to 0, and the shear-thinning behavior becomes more pronounced with increasing φ, as indicated by the parameters presented in Table 4. It is important to note that the power-law model is suitable for low solid concentrations (φ1 - φ3), with R^2 values > 0.96, but is not adequate at higher solid concentrations (φ4 - φ5).

To better understand the characteristics of the materials being examined, the apparent transitional yield stress as a function of the solid mass fraction has been determined (Fig. 9) using the continuous shear stress or shear rate ramp (depicted in Fig. S3) from low to high stress or rate, as previously reported (Mustafa et al., 2018).

The apparent transitional yield stress is an important characteristic of structured fluids because it provides an indication of gel stability. Higher apparent transitional yield stress for φ4 and φ5 (mass fraction of 25% and 30% w/w of WM in oil, respectively) suggests a more compact structure that prevents phase separation, sedimentation or aggregation due to stronger particle-particle interactions and the formation of a strong particle network. In conclusions, the results of Fig. 9 suggest that oil suspensions can be efficiently structured when the mass fraction of WM is higher than 20% w/w.

3.5. *Wheat middlings-in-oil-suspensions in the presence of water*

The addition of a secondary fluid with high affinity for solid particles, such as water, can significantly affect the gel structure. To investigate the interactions of the HSM- and HPH-treated WM particles with the secondary fluid in the presence of oil as a continuous phase, three-phase contact angles were measured (Fig. 10).

The three-phase contact angle curves recorded over 60 s were fitted with an exponential decay equation (Equation (7)):

$$\theta = \theta_\infty + (\theta_0 - \theta_\infty)\, e^{-\frac{t}{\tau_T}} \qquad \text{(Eq. 7)}$$

where Θ_0 is the initial contact angle, Θ_∞ is the asymptotic contact angle

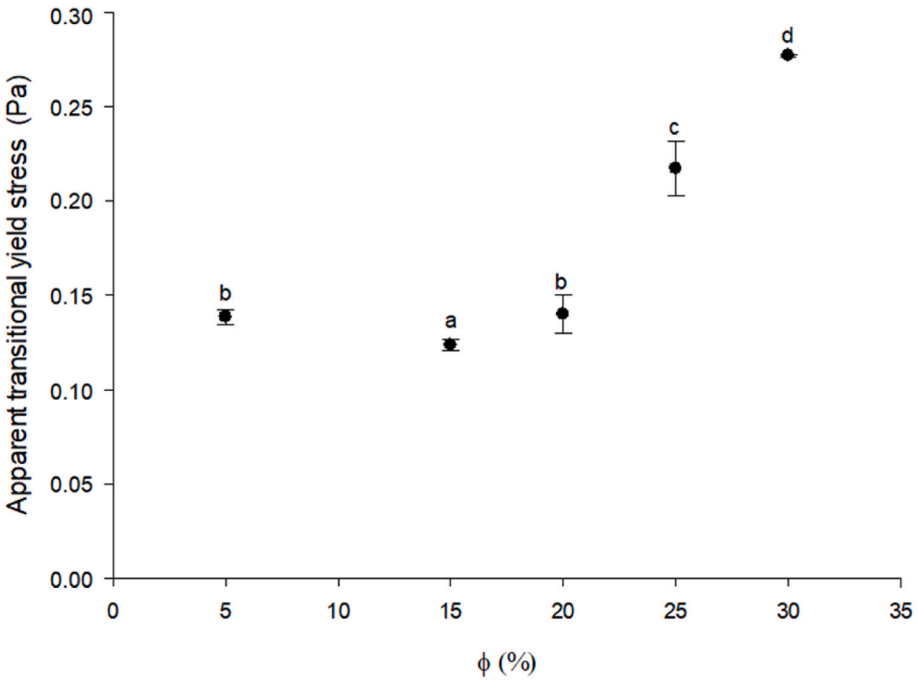

Fig. 9. Apparent transitional yield stress for WM-in-oil-suspensions as a function of solid mass fractions. Different letters denote statistically significant ($p < 0.05$) differences.

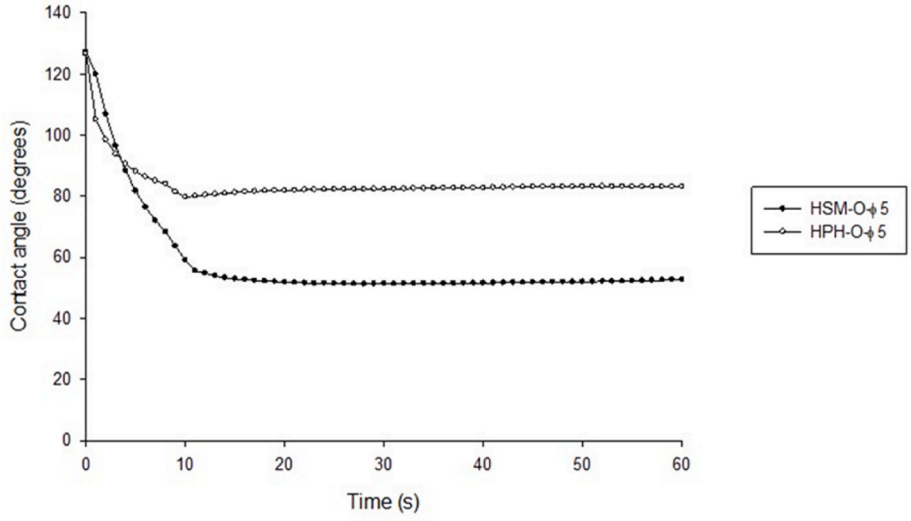

Fig. 10. Contact angle curves for HSM (–●–) and HPH (–○–) treated WM-in-oil-suspensions at φ = 30% w/w of particle mass fraction. Each curve is the average of three measurements.

Table 5
Three-phase contact angle parameters of the WM-in-oil-suspensions (φ = 30% w/w) treated by HSM and HPH.

	HSM-O-φ5	HPH-O-φ5
θ_0	132.18°	124.83°
θ_∞	51.12°	82.50°
τ_r	4.87 s	2.10 s
R^2	0.9936	0.9868
Adj-R^2	0.9873	0.9738

and τ_r is the characteristic time for the arrangement of the water droplet on WM particles at the oil interface, and t is the time variable. The fitting parameters for the curves in Fig. 10 are reported in Table 5.

In general, the contact angle Θ is a quantitative measure of the liquid's wetting capability on a solid: $\Theta < 90°$ indicates good wetting of the solid by the liquid, $\Theta \approx 90°$ indicates that the liquid spreads on the solid surface, and $\Theta > 90°$ represents a non-wetting condition. As expected, WM particles have a three-phase contact angle with oil and water that is lower than 90°, consistent with the hydrophilic nature of the organic polymeric chains that make up WM. This implies that WM suspensions in oil are arranged in a pendular state upon water addition (Koos, 2014). The three-phase contact angle for HSM-treated WM particles decreased from an initial value of 132.2° to an asymptotic value of 51.1°, following an exponential decay trend (Equation (7)). In contrast, the contact angle for HPH-treated WM particles tended towards an asymptotic value of 90°. These differences may be due to the different mechanical treatments applied to WM-in-oil-suspensions. It is possible that HPH

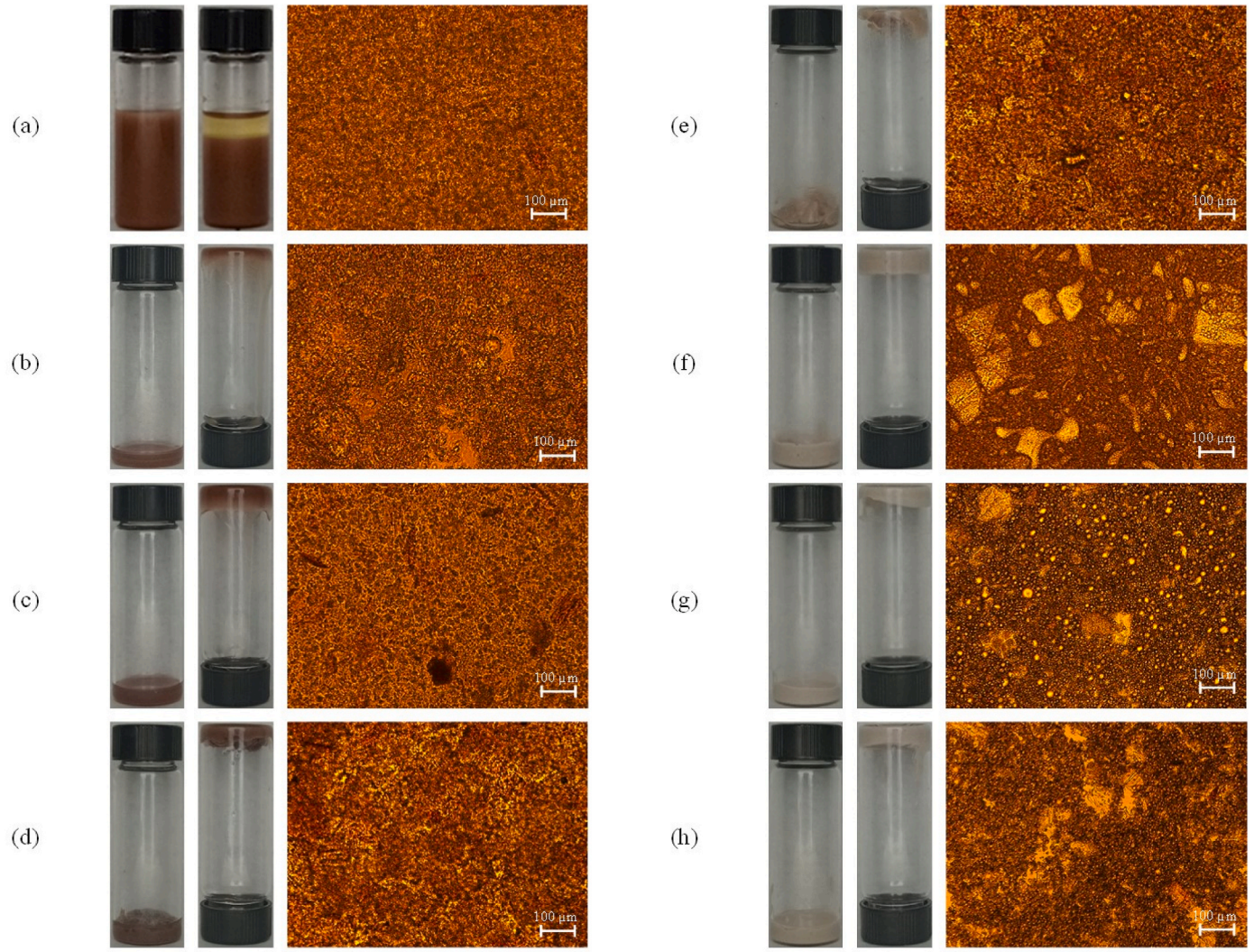

Fig. 11. Visual appearance and microscopic images of HPH suspensions prepared from HPH-O-φ5 at varying water addition: (a) S = 0.00; (b) S = 0.05; (c) S = 0.15; (d) S = 0.30; (e) S = 0.40; (f) S = 0.50; (g) S = 0.60; (h) S = 0.70. Panel (a) does not show the inverted bottle, unlike the other pictures, due to the low viscosity of the samples, causing them to flow excessively quickly to the bottom.

treatment increased porosity and allowed oil, in which WM is dispersed, to interact with hydrophobic parts of the particles, leading to their partial saturation (Ulbrich & Flöter, 2014). In contrast, porous effects were less pronounced for HSM-treated systems. However, this different behavior did not appear to negatively affect the water binding ability of HPH-treated WM particles.

3.6. Capillary suspensions characterization

The addition of water as a secondary fluid into HPH-O-φ5 (WM-in-oil-suspension at φ = 0.30 w/w treated with HPH, approximately at full saturation of oil holding capacity) was used to promote the formation of capillary suspensions through the development of capillary bridges and a 3D network.

3.6.1. Microstructural analysis

A capillary network forms when a secondary fluid (e.g. water) is added to a particle suspension in an immiscible fluid (e.g. oil), where the particle surface exhibits affinity for the secondary fluid (e.g. predominantly hydrophilic nature of the particle surface). The formation of a capillary suspension is accompanied by a transition from fluid-like to gel-like behavior, with increased consistency and firmness as the saturation ratio *S* increases, as shown in Fig. 11.

The sample at S = 0.05 (FOH ~ 5%, Table S1 in Supplementary Material) exhibited a very weak gel-like behavior, similar to the HPH-O-φ5 sample (S = 0.00). The micrographs for these two samples are also very similar (Fig. 11a and b), with no interconnected water-rich aggregates observed. As water addition increased, small water-rich aggregates, indicated by enlarged dark area in the microscopic images, were formed. For even higher water addition (S = 0.50), a very compact homogeneous structure was obtained, where water acted as a ligand for particle cluster formation. The formed clusters, with a size often exceeding 100 µm, could entrap the oil phase, forming a homogeneous gel. For S = 0.50, the fractional water holding FWH was approximately 100% (Table S1), which means that the solid water holding capacity reached the saturation value (WH_{max}) and the system was approaching phase inversion. The values of FWH for the different conditions investigated are reported in Table S1 of the Supplementary Material. WM-in-oil-suspensions with S > 0.50 (FWH ≫ 100%) exhibited the formation of oil droplets in the aqueous phase, suggesting phase inversion (Fig. 11g and h). This effect was previously reported by Calabrese et al., where oil-in-water emulsion droplets were observed for S = 0.40 (Calabrese et al., 2021). Overall, the enhanced gel-like behavior and formation of a capillary bridges network upon water addition strongly suggest that capillary forces control the rheological behavior of the ternary blend (Calabrese et al., 2021).

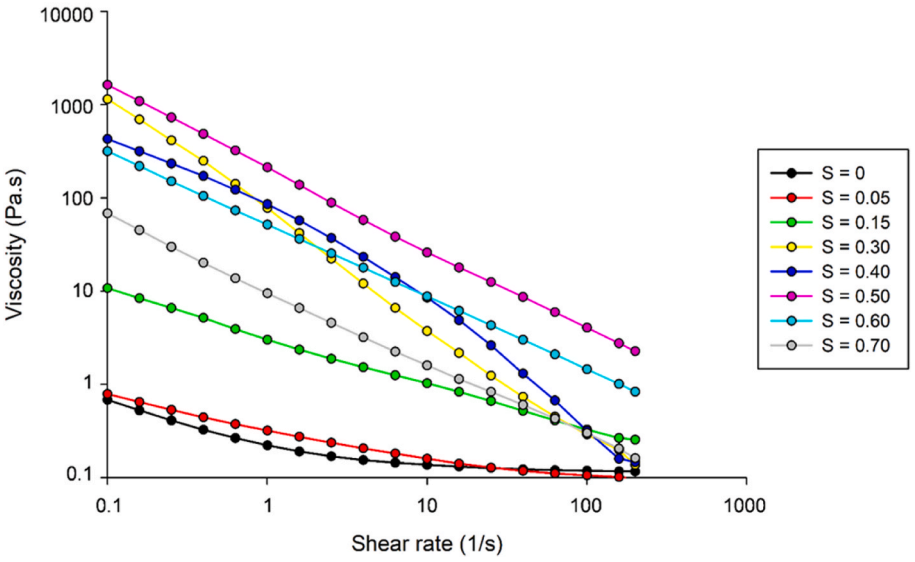

Fig. 12. Flow curves for HPH treated WM-in-oil-suspensions at φ = 30% w/w as a function of saturation degree.

Table 6
Fitting parameters and coefficients of determination for the fitting of the data of Fig. 12, using Equation (6).

	k (Pa·s^n)	n (-)	R^2	Adj-R^2
S = 0.00	0.25	1.46	0.9848	0.9840
S = 0.05	0.35	1.37	0.9941	0.9932
S = 0.15	1.57	1.80	0.9940	0.9934
S = 0.30	174.28	1.89	0.9940	0.9934
S = 0.40	55.13	1.85	0.9974	0.9970
S = 0.50	286.55	1.79	0.9971	0.9970
S = 0.60	29.67	1.97	0.9971	0.9970
S = 0.70	7.64	1.92	0.9990	0.9982

3.6.2. *Rheological properties*

The rheological behavior of the resulting capillary suspensions is shown in Fig. 12. Consistent with the micrographs of Fig. 11, the flow curves in Fig. 12 and Fig. S2 b demonstrate the formation of a capillary network structure that becomes stronger with increasing saturation ratio up to 50%, which can be explained by the formation of swollen aggregates interconnected via a 3D network.

Compared to the black curve, representing the oil suspension without water addition, which has lower viscosity values than all the other samples, the addition of water caused a measurable and significant increase in viscosity. All samples exhibited a shear-thinning behavior, which was most pronounced for S = 0.50, when most of the added water led to the formation of a bridge network, as indicated by the parameters

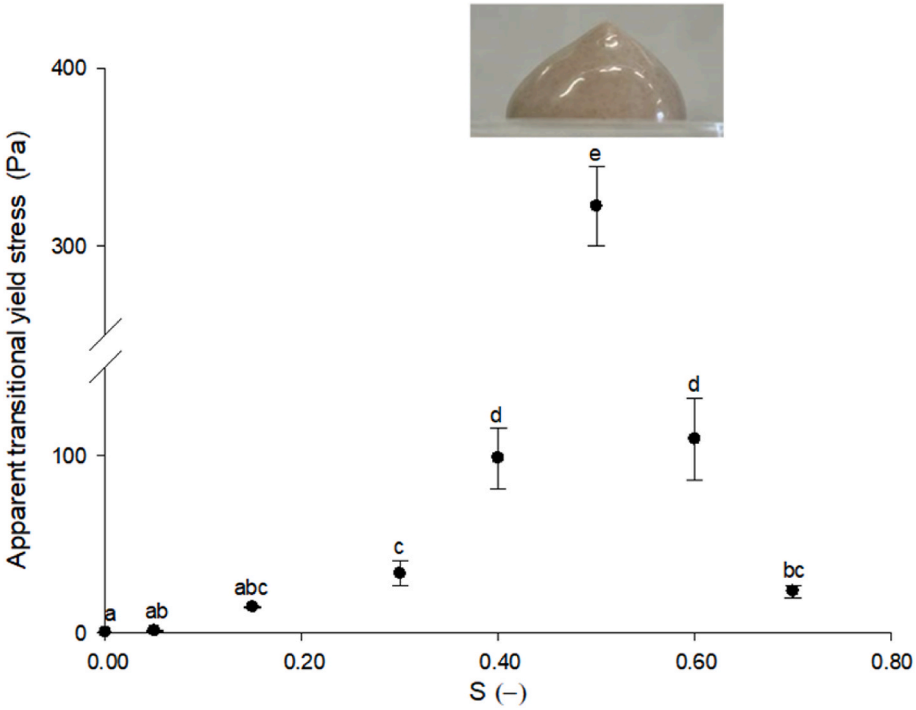

Fig. 13. Apparent transitional yield stress for WM-in-oil-suspensions at φ = 30% w/w as a function of saturation degree. Different letters denote statistically significant ($p < 0.05$) differences. On the top the visual image of capillary suspension at S = 0.50.

presented in Table 6. This state, called funicular (Wang et al., 2017), is typically disrupted at higher shear rates, as shown in Fig. 12.

Since WM particles are preferentially wetted by water, particle swelling and the capillary forces between neighboring particles are expected to play a dominant role in the rheological behavior of the mixtures (Koos & Willenbacher, 2011). The capillary suspension at S = 0.30 displayed high viscosity at low shear rates, followed by a rapid decrease with increasing shear rate, even at values lower than the sample with S = 0.15. This behavior could be explained by examining the image in Fig. 11d: the sample exhibits high inhomogeneity that may be associated with the formation of a pendular state, where formed bridges increase viscosity but are not strong enough to form a network that does not break during testing. Similar behavior was observed for the sample with saturation ratio S = 0.40, although the flow curve for the sample appears slightly lower than that at S = 0.30 for a shear rate $<1\ s^{-1}$. This difference can be attributed to the lack of homogeneity in the sample, leading to incomplete fragmentation during the rheological analysis at low shear rates. However, it is important to emphasize that for shear rates between 1 and 100 s^{-1}, a general monotonous trend is evident with increasing viscosity and a corresponding rise in the apparent transitional yield stress, shown in Fig. 13 as a function of saturation ratio, peaking at S = 0.50. The subsequent decrease in the apparent transitional yield stress can be attributed to the inversion of the continuous phase, which can significantly influence the overall rheological behavior of the system.

The addition of water dramatically changed the propriety of the suspension, as indicated by the apparent transitional yield stress, which increased progressively with water content due to increased network strength, reaching a maximum value at S = 0.50. At higher S values, the apparent transitional yield stress decreased, suggesting phase inversion. Notably, the apparent transitional yield stress at S = 0.50 was three orders of magnitude higher than for particle in oil suspension (S = 0.00). This value corresponds to the peak yield stress, indicating the formation of a network, in which water acts as a bridge between particles to form capillary bridges that are much stronger than the Van Der Waals forces acting in a simple suspension (Koos & Willenbacher, 2011). These results are consistent with other studies, where capillary suspensions exhibit an increase in apparent yield stress with increasing amounts of added secondary fluid (Calabrese et al., 2021; Mustafa et al., 2018), until maximum apparent yield stress is achieved at a saturation ratio of 0.50.

4. Conclusions

This study demonstrated for the first time that wheat middlings agri-food residues can be used to structure sunflower oil. It also showed that the HPH mechanical treatment (80 MPa for 20 equivalent passes) can be applied directly to the wheat middling particles in oil to efficiently break-up particles and activate fibers, which is important for the formation of capillary bridges and a three-dimensional network that regulates the apparent viscosity and apparent transitional yield stress of the capillary suspension, when water is added as a secondary fluid. Therefore, oil structuring with HPH-treated wheat middling may support the development of more sustainable and health-beneficial olecolloids as replacements for solid fats, enabling the reduction of the caloric content and increase in dietary fiber content, while also exploiting the recovery of valuable bioactive compounds present in the residues. These antioxidant compounds released into the suspension can reduce the oxidation of sunflower oil used in capillary suspensions due to the water addition. Further studies are needed to explore the application of these oleocolloids capillary suspensions in spreads, creams, fillings or baking applications to evaluate the quality of these new products in terms of texture (how the new low-fat food products can mimick the texture of regular full-fat products), *in vitro* digestion, microbial stability, and organoleptic properties.

Funding

This research was funded by the Italian Ministry of University (MUR) call PRIN 2017 with the project 2017LEPH3M "PANACEA: A technology PlAtform for the sustainable recovery and advanced use of NAnostructured CEllulose from Agro-food residues".

This study was also carried out within the Agritech National Research Center and received funding from the European Union NextGenerationEU (PIANO NAZIONALE DI RIPRESA E RESILIENZA (PNRR) – MISSIONE 4 COMPONENTE 2, INVESTIMENTO 1.4 – D.D. 1032 17/06/2022, CN00000022). This manuscript reflects only the authors' views and opinions, neither the European Union nor the European Commission can be considered responsible for them.

CRediT authorship contribution statement

Annachiara Pirozzi: Conceptualization, Methodology, Formal analysis, Investigation, Resources, Writing – original draft, preparation, Writing – review & editing. **Alfredo Posocco:** Formal analysis, Investigation. **Francesco Donsì:** Methodology, Supervision, Resources, Writing – review & editing, Funding acquisition, All authors have read and agreed to the published version of the manuscript.

Declaration of competing interest

The authors declare the following financial interests/personal relationships which may be considered as potential competing interests: Francesco Donsi' reports financial support was provided by Government of Italy Ministry of Education University and Research.

Data availability

Data will be made available on request.

Acknowledgments

The authors kindly thank Luigi Esposito for particle size measurements.

Appendix A. Supplementary data

Supplementary data to this article can be found online at https://doi.org/10.1016/j.foodhyd.2023.109152.

References

Bagnasco, L., Pappalardo, V. M., Meregaglia, A., Kaewmanee, T., Ubiali, D., Speranza, G., & Cosulich, M. E. (2013). Use of food-grade proteases to recover umami protein-peptide mixtures from rice middlings. *Food Research International, 50*(1), 420–427. https://doi.org/10.1016/j.foodres.2012.11.007

Bealer, E. J., Onissema-karimu, S., Rivera-galletti, A., Francis, M., Wilkowski, J., & Hu, X. (2020). Protein – polysaccharide composite materials: Fabrication and applications. *Polymers, 12*(2), 464. https://doi.org/10.3390/polym12020464

Begum, H. A., Tanni, T. R., & Shahid, M. A. (2021). Analysis of water absorption of different natural fibers. *Journal of Textile Science and Technology, 7*, 152–160. https://doi.org/10.4236/jtst.2021.74013

Benzie, I. F. F., & Strain, J. J. (1996). The ferric reducing ability of plasma (FRAP) as a measure of "antioxidant power": The FRAP assay. *Analytical Biochemistry, 239*, 70–76. https://doi.org/10.1006/abio.1996.0292

Bossler, F., Weyrauch, L., Schmidt, R., & Koos, E. (2017). Influence of mixing conditions on the rheological properties and structure of capillary suspensions. *Colloids and Surfaces A: Physicochemical and Engineering Aspects, 518*, 85–97. https://doi.org/10.1016/j.colsurfa.2017.01.026

Calabrese, V., Gunes, D. Z., & Farrés, I. F. (2021). Rheological control of pea fibre dispersions in oil: The role of particle and water volume fractions. *Food Hydrocolloids, 121*, Article 106988. https://doi.org/10.1016/j.foodhyd.2021.106988

Chau, C. F., Wang, Y. T., & Wen, Y. L. (2007). Different micronization methods significantly improve the functionality of carrot insoluble fibre. *Food Chemistry, 100*, 1402–1408. https://doi.org/10.1016/j.foodchem.2005.11.034

Chen, J., Gao, D., Yang, L., & Gao, Y. (2013). Effect of microfluidization process on the functional properties of insoluble dietary fiber. *Food Research International, 54*, 1821–1827. https://doi.org/10.1016/j.foodres.2013.09.025

Coccaro, N., Ferrari, G., & Donsì, F. (2018). Understanding the break-up phenomena in an orifice-valve high pressure homogenizer using spherical bacterial cells (Lactococcus lactis) as a model disruption indicator. *Journal of Food Engineering, 236*, 60–71. https://doi.org/10.1016/J.JFOODENG.2018.05.011

Cromwell, G. L., Cline, T. R., Crenshaw, J. D., Crenshaw, T. D., Easter, R. A., Ewan, R. C., Hamilton, C. R., Hill, G. M., Lewis, A. J., Mahan, D. C., Nelssen, J. L., Pettigrew, J. E., Veum, T. L., & Yen, J. T. (2000). Variability among sources and laboratories in analyses of wheat middlings. *Journal of Animal Science, 78*, 2652–2658. https://doi.org/10.2527/2000.78102652x

Damodaran, S., & Paraf, A. (2017). Food proteins and their applications. In *Protein-lipid and protein-flavor interactions* (1st ed.). https://doi.org/10.1201/9780203755617 (Chapter 5)).

De Vasconcelos, M. C. B. M., Bennett, R., Castro, C., Cardoso, P., Saavedra, M. J., & Rosa, E. A. (2013). Study of composition, stabilization and processing of wheat germ and maize industrial by-products. *Industrial Crops and Products, 42*(1), 292–298. https://doi.org/10.1016/j.indcrop.2012.06.007

Elleuch, M., Bedigian, D., Roiseux, O., Besbes, S., Blecker, C., & Attia, H. (2011). Dietary fibre and fibre-rich by-products of food processing: Characterisation, technological functionality and commercial applications: A review. *Food Chemistry, 124*, 411–421. https://doi.org/10.1016/j.foodchem.2010.06.077

Ferrari, G., Mustafa, W., & Donsì, F. (2017). Use of agri-food residues for oil structuring and functionalization. *Chemical Engineering Transactions, 57*, 1831–1836. https://doi.org/10.3303/CET1757306

Fleury, N., & Lahaye, M. (1991). Chemical and physico-chemical characterisation of fibres from laminaria digitata (kombu Breton): A physiological approach. *Journal of the Science of Food and Agriculture, 55*, 389–400. https://doi.org/10.1002/jsfa.2740550307

Galanakis, C. M. (2018). Sustainable recovery and reutilization of cereal processing by-products. In *Concluding remarks and future perspectives* (1st ed.). https://doi.org/10.1016/B978-0-08-102162-0.00011-3 (Chapter 11)).

Ghosh, S., & Rousseau, D. (2011). Fat crystals and water-in-oil emulsion stability. *Current Opinion in Colloid & Interface Science, 16*, 421–431. https://doi.org/10.1016/j.cocis.2011.06.006

Goh, K. K. T., Kumar, R., & Wong, S. S. (2014). Functionality of non-starch polysaccharides (NSPs). *Functional Foods and Dietary Supplements: Processing Effects and Health Benefits, 9781118227*, 187–225. https://doi.org/10.1002/9781118227800.ch8

Grigelmo-Miguel, N., & Martín-Belloso, O. (1999). Characterization of dietary fiber from orange juice extraction. *Food Research International, 31*, 355–361. https://doi.org/10.1016/S0963-9969(98)00087-8

Hodson, L., Skeaff, C. M., & Chisholm, W. A. H. (2001). The effect of replacing dietary saturated fat with polyunsaturated or monounsaturated fat on plasma lipids in free-living young adults. *European Journal of Clinical Nutrition, 55*, 908–915. https://doi.org/10.1038/sj.ejcn.1601234

Hoffmann, S., Koos, E., & Willenbacher, N. (2014). Using capillary bridges to tune stability and flow behavior of food suspensions. *Food Hydrocolloids, 40*, 44–52. https://doi.org/10.1016/j.foodhyd.2014.01.027

Huang, L., Liu, J., Addy, M., Ding, B., Cheng, Y., Peng, P., Wang, Y., Liu, Y., Chen, P., & Ruan, R. (2020). Physicochemical and emulsifying properties of orange fibers stabilized oil-in-water emulsions. *Lebensmittel-Wissenschaft und -Technologie, 133*, Article 110054. https://doi.org/10.1016/j.lwt.2020.110054

Huang, Q., Shi, C. X., Su, Y. B., Liu, Z. Y., Li, D. F., Liu, L., Huang, C. F., Piao, X. S., & Lai, C. H. (2014). Prediction of the digestible and metabolizable energy content of wheat milling by-products for growing pigs from chemical composition. *Animal Feed Science and Technology, 196*, 107–116. https://doi.org/10.1016/j.anifeedsci.2014.06.009

Hu, R., Zhang, M., Adhikari, B., & Liu, Y. (2015). Effect of homogenization and ultrasonication on the physical properties of insoluble wheat bran fibres. *International Agrophysics, 29*(4), 423–432. https://doi.org/10.1515/intag-2015-0048

Jurić, S., Ferrari, G., Velikov, K. P., & Donsì, F. (2019). High-pressure homogenization treatment to recover bioactive compounds from tomato peels. *Journal of Food Engineering, 262*, 170–180. https://doi.org/10.1016/j.jfoodeng.2019.06.011

Koos, E. (2014). Capillary suspensions: Particle networks formed through the capillary force. *Current Opinion in Colloid & Interface Science, 19*, 575–584. https://doi.org/10.1016/j.cocis.2014.10.004

Koos, E., Johannsmeier, J., Schwebler, L., & Willenbacher, N. (2012). Tuning suspension rheology using capillary forces. *Soft Matter, 8*, 6620–6628. https://doi.org/10.1039/c2sm25681a

Koos, E., & Willenbacher, N. (2011). Capillary forces in suspension rheology. *Science, 331*, 897–900. https://doi.org/10.1126/science.1199243

Kosseva, M. R. (2020). Food industry wastes. In *Sources, characteristics and treatment of plant-based food waste* (2nd ed.). https://doi.org/10.1016/b978-0-12-817121-9.00003-6 (Chapter 3)).

Le Révérend, B. J. D., Norton, I. T., Cox, P. W., & Spyropoulos, F. (2010). Colloidal aspects of eating. *Current Opinion in Colloid & Interface Science, 15*, 84–89. https://doi.org/10.1016/j.cocis.2009.11.009

Liu, A. G., Ford, N. A., Hu, F. B., Zelman, K. M., Mozaffarian, D., & Kris-Etherton, P. M. (2017). A healthy approach to dietary fats: Understanding the science and taking action to reduce consumer confusion. *Nutrition Journal, 16*, 53. https://doi.org/10.1186/s12937-017-0271-4

Mewis, J., & Wagner, N. J. (2011). Colloidal suspension rheology. In *Rheometry of suspensions* (1st ed.). https://doi.org/10.1017/CBO9780511977978 (Chapter 9)).

Mustafa, W., Pataro, G., Ferrari, G., & Donsì, F. (2018). Novel approaches to oil structuring via the addition of high-pressure homogenized agri-food residues and water forming capillary bridges. *Journal of Food Engineering, 236*, 9–18. https://doi.org/10.1016/j.jfoodeng.2018.05.003

Pirozzi, A., Capuano, R., Avolio, R., Gentile, G., Ferrari, G., & Donsì, F. (2021). O/W Pickering emulsions stabilized with cellulose nanofibrils produced through different mechanical treatments. *Foods, 10*, 1886. https://doi.org/10.3390/foods10081886

Pirozzi, A., Ferrari, G., & Donsì, F. (2022). Cellulose isolation from tomato pomace pretreated by high-pressure homogenization. *Foods, 11*, 266. https://doi.org/10.3390/foods11030266

Principato, L., Carullo, D., Bassani, A., Spigno, G., Gruppi, A., Duserm Garrido, G., & Dordoni, R. (2021). Effect of dietary fiber and thermal conditions on rice bran wax-based structured edible oils. *Foods, 10*(12), 3072. https://doi.org/10.3390/foods10123072

Rosenfelder, P., Eklund, M., & Mosenthin, R. (2013). Nutritive value of wheat and wheat by-products in pig nutrition: A review. *Animal Feed Science and Technology, 185*, 107–125. https://doi.org/10.1016/j.anifeedsci.2013.07.011

Rousseau, D. (2000). Fat crystals and emulsion stability - a review. *Food Research International, 33*, 3–14. https://doi.org/10.1016/S0963-9969(00)00017-X

Rousseau, D., & Hodge, S. M. (2005). Stabilization of water-in-oil emulsions with continuous phase crystals. *Colloids and Surfaces A: Physicochemical and Engineering Aspects, 260*, 229–237. https://doi.org/10.1016/j.colsurfa.2005.02.035

Ryoo, J. H., Ha, E. H., Kim, S. G., Ryu, S., & Lee, D. W. (2011). Apolipoprotein B is highly associated with the risk of coronary heart disease as estimated by the framingham risk score in healthy Korean men. *Journal of Korean Medical Science, 26*, 631–636. https://doi.org/10.3346/jkms.2011.26.5.631

Shajahan, T., & Paul, W. (2020). Influence of concentration on sedimentation of a dense suspension in a viscous fluid. *Flow, Turbulence and Combustion, 105*(2), 537–554. https://doi.org/10.1007/s10494-020-00172-8

Slinkard, K., & Singleton, V. (1977). Total phenol analysis: Automation and comparison with manual methods. *American Journal of Enology and Viticulture, 28*, 49–55. https://doi.org/10.5344/ajev.1974.28.1.49

Stanton, J., Xue, Y., Pandher, P., Malek, L., Brown, T., Hu, X., & Salas-de la Cruz, D. (2018). Impact of ionic liquid type on the structure, morphology and properties of silk-cellulose biocomposite materials. *International Journal of Biological Macromolecules, 108*, 333–341. https://doi.org/10.1016/j.ijbiomac.2017.11.137

Stevenson, L., Phillips, F., O'sullivan, K., & Walton, J. (2012). Wheat bran: Its composition and benefits to health, a European perspective. *International Journal of Food Sciences & Nutrition, 63*(8), 1001–1013. https://doi.org/10.3109/09637486.2012.687366

Su, D., Zhu, X., Wang, Y., Li, D., & Wang, L. (2019). Effects of high-pressure homogenization on physical and thermal properties of citrus fiber. *Lebensmittel-Wissenschaft und -Technologie, 116*, Article 108573. https://doi.org/10.1016/j.lwt.2019.108573

Technical Association of Pulp and Paper Industry (TAPPI). (2006). *Standard: TAPPI T-222 om-22. Acid-insoluble lignin in wood and pulp*.

Technical Association of Pulp and Paper Industry (TAPPI). (2007). *Standard: TAPPI T-264 cm-07. Preparation of wood for chemical analysis*.

Ulbrich, M., & Flöter, E. (2014). Impact of high pressure homogenization modification of a cellulose based fiber product on water binding properties. *Food Hydrocolloids, 41*, 281–289. https://doi.org/10.1016/j.foodhyd.2014.04.020

de Vries, A., Jansen, D., van der Linden, E., & Scholten, E. (2018). Tuning the rheological properties of protein-based oleogels by water addition and heat treatment. *Food Hydrocolloids, 79*, 100–109. https://doi.org/10.1016/j.foodhyd.2017.11.043

Wang, J. P., Gallo, E., François, B., Gabrieli, F., & Lambert, P. (2017). Capillary force and rupture of funicular liquid bridges between three spherical bodies. *Powder Technology, 305*, 89–98. https://doi.org/10.1016/j.powtec.2016.09.060

Yuan, Z., Zhu, D., Xu, X., Xu, J., Yang, L., Song, H., Wang, S., Liu, J., & Liu, H. (2023). Homogenized soybean hull suspension as an emulsifier for oil/water emulsions: Synergistic effect of the insoluble fiber and soluble polysaccharide. *International Journal of Biological Macromolecules, 237*, Article 123950. https://doi.org/10.1016/j.ijbiomac.2023.123950

Yue, L., Shoemaker, C. F., Xueran, S., Jianguo, M., Ibáñez-Carranza, A. M., & Fang, Z. (2008). The isolation of rice starch with food grade proteases combined with other treatments. *Food Science and Technology International, 14*(3), 215–224. https://doi.org/10.1177/1082013208092824